EXCLI Journal 2017;16:1114-1131 – ISSN 1611-2156
Received: February 10, 2017, accepted: July 31, 2017, published: August 30, 2017

Original article:

MICROWAVE-ASSISTED SYNTHESIS AND ANTITUMOR EVALUATION OF A NEW SERIES OF THIAZOLYLCOUMARIN DERIVATIVES

Moustafa T. Gabr[a,b], Nadia S. El-Gohary[a*], Eman R. El-Bendary[a], Mohamed M. El-Kerdawy[a], Nanting Ni[b]

[a] Department of Medicinal Chemistry, Faculty of Pharmacy, Mansoura University, Mansoura 35516, Egypt
[b] Department of Chemistry, Georgia State University, Atlanta, Georgia 30303, USA

[*] Corresponding author: Nadia S. El-Gohary, Department of Medicinal Chemistry, Faculty of Pharmacy, Mansoura University, Mansoura 35516, Egypt; Tel.: +2 010 00326839; Fax: +2 050 2247496; E-mail: dr.nadiaelgohary@yahoo.com

http://dx.doi.org/10.17179/excli2017-208

ABSTRACT

A new series of thiazolylcoumarin derivatives was synthesized. The designed strategy embraced a molecular hybridization approach which involves the combination of the thiazole and coumarin pharmacophores together. The new hybrid compounds were tested for *in vitro* antitumor efficacy over cervical (Hela) and kidney fibroblast (COS-7) cancer cells. Compounds **5f**, **5h**, **5m** and **5r** displayed promising efficacy toward Hela cell line. In addition, **5h** and **5r** were found to be the most active candidates toward COS-7 cell line. The four active analogs, **5f**, **5h**, **5m** and **5r** were screened for *in vivo* antitumor activity over EAC cells in mice, as well as *in vitro* cytotoxicity toward W138 normal cells. Results illustrated that **5r** has the highest *in vivo* activity, and that the four analogs are less cytotoxic than 5-FU toward W138 normal cells. In this study, 3D pharmacophore analysis was performed to investigate the matching pharmacophoric features of the synthesized compounds with trichostatin A. *In silico* studies showed that the investigated compounds meet the optimal needs for good oral absorption with no expected toxicity hazards.

Keywords: thiazolylcoumarins, synthesis, antitumor activity, cytotoxic activity, 3D pharmacophore elucidation, *in silico* studies

INTRODUCTION

Cancer is a collection of related diseases. Cancer cells can metastasize and invade nearby tissues through blood stream or lymphatic system (Bagi, 2002). In general, cancer develops as a result of genetic changes, such as mutations in DNA. Cancer treatment includes radiation therapy, gene therapy and chemotherapy. Ideal anticancer agents would kill cancer cells without affecting normal tissues. Therefore, the evolution of new safe anticancer agents is a serious task for medicinal chemists.

Histone deacetylases (HDACs) are Zn^{2+} dependent enzymes that catalyze the deacetylation of lysine residues located at the N-ε terminal extensions of core histones resulting in chromatin condensation and transcriptional repression (Kouzarides, 2007). Eleven isoforms of HDACs are present in human (Gregoretti et al., 2004). Abnormalities in the deacetylation function of histones were recognized in various human tumors (Falkenberg and Johnstone, 2014).

EXCLI Journal 2017;16:1114-1131 – ISSN 1611-2156
Received: February 10, 2017, accepted: July 31, 2017, published: August 30, 2017

Most HDACs inhibitors share common pharmacophoric features which can be exemplified by trichostatin A, a natural HDACs inhibitor. The common pharmacophore is composed of three regions: zinc binding group (ZBG) that chelates Zn^{2+} at the active site of the enzyme, cap group which binds to the surface of the active pocket and a linker between the ZBG and the cap group (Feng et al., 2013). Literature survey revealed the significance of variations in the cap group (Bowers et al., 2009a, b) and the linker (Weerasinghe et al., 2008) on the HDACs inhibitory activity. However, the type of ZBG is believed to greatly affect the potency and isoform selectivity of HDACs inhibitors (Methot et al., 2008). Hydroxamic acid moiety is a typical ZBG which is common in numerous HDACs inhibitors. Due to the drawbacks of hydroxamate functional group which include non-specific inhibition of all HDAC isoforms (Day and Cohen, 2013), diverse moieties such as thiols, benzamides, sulphamides and trithiocarbonates were incorporated into diverse scaffolds and investigated for their capability as ZBG (Chen et al., 2013; Di Micco et al., 2013; Kawai and Nagata, 2012). Methyl ketone was utilized as ZBG in the design of HDACs inhibitors (Ilies et al., 2011). Analogously, we introduced coumarin moiety as a novel ZBG in the design of new HDACs inhibitors aiming to explore its effect as a non-hydroxamate functional group. The hydrazinylthiazole in the synthesized hybrids is implied as a linker which projects the ZBG into the active site of HDACs. The cap region in the common pharmacophore has a strong contribution to the overall binding affinity of HDACs inhibitors (Salisbury and Cravatt, 2007). The common pharmacophoric features of trichostatin A and the proposed thiazolylcoumarin hybrids are illustrated in Figure 1.

Literature revealed that numerous HDACs inhibitors have antitumor activity (Zain et al., 2010). Most of the reported HDACs inhibitors are hydroxamic acid derivatives that exhibit non-specific inhibition of all HDAC isoforms (Day and Cohen, 2013). As a result, extensive research is directed toward the development of non-hydroxamate HDACs inhibitors (Madsen et al., 2014).

Coumarins of natural and synthetic origins constitute an important class of compounds. They were proved to possess significant therapeutic potential, including antitumor activity (Morsy et al., 2017; Emami and Dadashpour, 2015; Klenkar and Molnar, 2015; Amin et al., 2015; Pingaew et al., 2014b; Sandhu et al., 2014; Liu et al., 2014; Li et al., 2014; Seidel et al., 2014; Sashidhara et al., 2010; Riveiro et al., 2010). On the same line, thiazole ring is a prominent skeleton in various bioactive molecules, including antitumor compounds (Tay et al., 2017; Gomha et al., 2015; Abouzeid and El-Subbagh, 2015; Nofal et al., 2014; Rouf and Tanyeli, 2015; Prashanth et al., 2014; Yuan et al., 2014; Shitre et al., 2014; Tung et al., 2013).

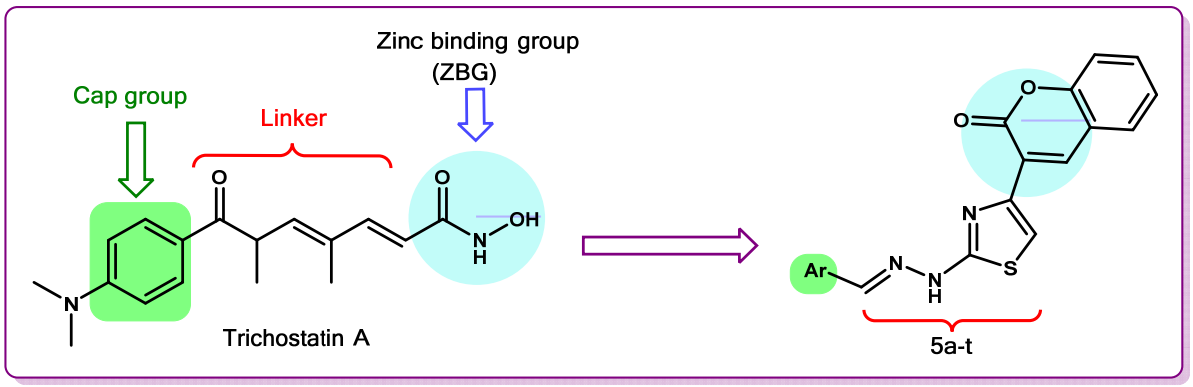

Figure 1: Common pharmacophoric features of trichostatin A and the proposed thiazolylcoumarin hybrids **5a-t**

EXCLI Journal 2017;16:1114-1131 – ISSN 1611-2156
Received: February 10, 2017, accepted: July 31, 2017, published: August 30, 2017

Moreover, literature survey indicated that thiazolylcoumarin hybrids (Abdul Rahman et al., 2016; Vaarla et al., 2015; Sreekanth et al., 2014; Srimanth et al., 2002) and other aryl(heteroaryl)coumarin hybrids (Zhang et al., 2017; Pangal et al., 2017; Luo et al., 2017; Garazd et al., 2017; Holiyachi et al., 2016; Goel et al., 2015; Zhang et al., 2014; Kamal et al., 2009; Ganina et al., 2008) have promising antitumor activity.

Hybrid approaches in drug design proved to offer advantages in drug-resistance (Hubschwerlen et al., 2003), introducing compounds with improved biological activity (Pingaew et al., 2014a) as well as their contribution in the development of promising agents with potent antitumor activity (Piens et al., 2014; Romagnoli et al., 2013). Therefore, we followed the hybridization strategy, combining the thiazole and coumarin pharmacophores together hoping to obtain new safe antitumor compounds. In addition, the design strategy embraced the profiling of diverse aromatic moieties (representing the cap group) on the thiazolylcoumarin scaffold in order to study the relationship between the interaction forces of the cap group to the target receptor and the antitumor activity of the proposed thiazolylcoumarin hybrids. The new hybrid compounds were assessed for *in vitro* antitumor activity, and the four active analogs, **5f**, **5h**, **5m** and **5r** were screened for *in vivo* antitumor activity over EAC in mice, as well as *in vitro* cytotoxicity toward W138 normal cells. HDACs inhibitory activity of the new active compounds is a plausible mechanism that might shed light toward the discovery of a new class of HDACs inhibitors.

MATERIALS AND METHODS

Chemistry

Stuart SMP10 melting point apparatus was utilized to determine melting points °C. Bruker Avance 400 MHz spectrometer was applied for recording ^{1}H and ^{13}C NMR spectra; chemical shifts are expressed in δ ppm with reference to TMS (Georgia State University, USA). HRMS were obtained on nano LC-Q-TOF spectrometer in +ve or -ve ion mode (Georgia State University, USA). Elemental analyses (C, H, N) were determined, and were within ± 0.4% of the calculated values (Georgia State University, USA). The completion of reactions was controlled utilizing TLC plates (silica gel 60 F254, Merck) and UV (366 nm) was used for visualization of the spots. Chloroform/methanol (9:1) and *n*-hexane/ethyl acetate (3:1) were utilized as elution solvents.

Synthesis of 3-acetylcoumarin (2): Salicylaldehyde **(1)** (2.20 g, 18 mmol), ethyl acetoacetate (3.12 g, 24 mmol) and piperidine (0.1 mL) were heated in ethanol (5 mL) under microwave irradiation (50 W) at 45 °C for 5 min. The precipitated solid upon cooling was filtered and crystallized from ethanol. Yield 85%, m.p. 117-118 °C (Valizadeh et al., 2007). ^{1}H NMR (DMSO-d_6) δ 2.40 (s, 2H, CH_2), 7.40-8.00 (m, 4H, Ar-H), 8.80 (s, 1H, C_4-H of chromone).

Synthesis of 3-(bromoacetyl)coumarin (3): A solution of bromine (1.60 g, 20 mmol) was added dropwise with constant stirring to a solution of compound **2** (2 g, 11 mmol) in chloroform (15 mL). The mixture was stirred at 0-5 °C for 6 hrs and the orange solid obtained was filtered and crystallized from glacial acetic acid. Yield 63%, m.p. 161-162 °C (Siddiqui et al., 2009). ^{1}H NMR (DMSO-d_6) δ 4.90 (s, 2H, CH_2), 7.40-8.00 (m, 4H, Ar-H), 8.80 (s, 1H, C_4-H of chromone).

Synthesis of 2-arylidenehydrazinocarbothioamides 4a-t: Thiosemicarbazide (0.092 g, 1 mmol), aromatic aldehyde (1 mmol) and glacial acetic acid (0.1 mL) were heated in ethanol (10 mL) under microwave irradiation (50 W) at 80 °C for 10 min. The precipitate formed upon cooling was filtered and crystallized to afford **4a-t**.

2-(2-Bromobenzylidene)hydrazinocarbothioamide (4a): Yield 84%, m.p. 202-203 °C (Coxon et al., 2013), (ethyl acetate/ethanol (3:1)), $C_8H_8BrN_3S$. ^{1}H NMR (DMSO-d_6) δ 7.25-8.45 (m, 7H, Ar-H, NH_2, CH=N), 11.65

(s, 1H, NH). ^{13}C NMR (DMSO-*d*$_6$) δ 124.0, 128.1, 128.2, 131.8, 133.3, 133.4, 141.2, 178.6.

2-(2-Cyanobenzylidene)hydrazinocarbothioamide (4b): Yield 91%, m.p. 212-213 °C (Hernandez et al., 2010), (chloroform), $C_9H_8N_4S$. ^{1}H NMR (DMSO-*d*$_6$) δ 7.60-8.55 (m, 7H, Ar-H, CH=N, NH_2), 11.85 (s, 1H, NH).

2-(3-Cyanobenzylidene)hydrazinocarbothioamide (4c): Yield 82%, m.p. 204-205 °C (Hernandez et al., 2008), (ethanol/water (2:1)), $C_9H_8N_4S$. ^{1}H NMR (DMSO-*d*$_6$) δ 7.55-8.45 (m, 7H, Ar-H, CH=N, NH_2), 11.60 (s, 1H, NH). ^{13}C NMR (DMSO-*d*$_6$) δ 112.1, 116.6, 130.2, 132.1, 133.7, 134.1, 134.6, 144.3, 177.9.

2-(4-(Trifluoromethyl)benzylidene)hydrazinocarbothioamide (4d): Yield 79%, m.p. 169-170 °C (Bernstein et al., 1951), (ethyl acetate/ethanol (3:1)), $C_9H_8F_3N_3S$. ^{1}H NMR (DMSO-*d*$_6$) δ 7.75-8.45 (m, 7H, Ar-H, NH_2, CH=N), 11.65 (s, 1H, NH). ^{13}C NMR (DMSO-*d*$_6$) δ 123.2, 125.8, 128.2, 130.0, 138.6, 144.2, 178.8.

2-(3-Methylbenzylidene)hydrazinocarbothioamide (4e): Yield 79%, m.p. 190-191 °C (Lv et al., 2010), (methanol), $C_9H_{11}N_3S$. ^{1}H NMR (DMSO-*d*$_6$) δ 2.45 (s, 3H, CH_3), 7.15-8.45 (m, 7H, Ar-H, NH_2, CH=N), 11.40 (s, 1H, NH). ^{13}C NMR (DMSO-*d*$_6$) δ 23.6, 125.7, 127.9, 129.2, 130.9, 133.6, 136.5, 144.1, 179.2.

2-(2,6-Dichlorobenzylidene)hydrazinocarbothioamide (4f): Yield 81%, m.p. 236-238 °C (Bernstein et al., 1951), (ethanol/water (2:1)), $C_8H_7Cl_2N_3S$. ^{1}H NMR (DMSO-*d*$_6$) δ 7.30-8.50 (m, 6H, Ar-H, CH=N, NH_2), 11.75 (s, 1H, NH).

2-(2-Chloro-6-fluorobenzylidene)hydrazinocarbothioamide (4g): Yield 85%, m.p. 241-242 °C (Sumangala et al., 2012), (ethyl acetate/ethanol (3:1)), $C_8H_7ClFN_3S$. ^{1}H NMR (DMSO-*d*$_6$) δ 7.20-8.45 (m, 6H, Ar-H, NH_2, CH=N), 11.75 (s, 1H, NH).

2-(2-Chloro-5-nitrobenzylidene)hydrazinocarbothioamide (4h): Yield 79%, m.p. 207-208 °C (Hao, 2010), (ethanol /water (2:1)), $C_8H_7ClN_4O_2S$. ^{1}H NMR (DMSO-*d*$_6$) δ 7.75-9.00 (m, 6H, Ar-H, CH=N, NH_2), 11.80 (s, 1H, NH). ^{13}C NMR (DMSO-*d*$_6$) δ 125.1, 125.8, 129.6, 133.9, 141.2, 145.1, 146.9, 179.1.

2-(3-Bromo-4-hydroxybenzylidene)hydrazinocarbothioamide (4i): Yield 67%, m.p. 169-172 °C (Tsurkan et al., 1982), (methanol), $C_8H_8BrN_3OS$. ^{1}H NMR (DMSO-*d*$_6$) δ 6.95-8.20 (m, 6H, Ar-H, NH_2, CH=N), 10.75 (s, 1H, OH), 11.30 (s, 1H, NH).

2-(2-Hydroxy-5-methylbenzylidene)hydrazinocarbothioamide (4j): Yield 72%, m.p. 196-198 °C (Pahontu et al., 2013), (ethyl acetate/ethanol (3:1)), $C_9H_{11}N_3OS$. ^{1}H NMR (DMSO-*d*$_6$) δ 2.20 (s, 3H, CH_3), 6.70-8.30 (m, 6H, Ar-H, NH_2, CH=N), 9.50 (s, 1H, OH), 11.30 (s, 1H, NH).

2-(4-Hydroxy-3-methylbenzylidene)hydrazinocarbothioamide (4k): Yield 71%, m.p. 173-175 °C, (ethyl acetate/ethanol (3:1)) (Kaishi, 1953), $C_9H_{11}N_3OS$. ^{1}H NMR (DMSO-*d*$_6$) δ 2.15 (s, 3H, CH_3), 6.85-8.05 (m, 6H, Ar-H, NH_2, CH=N), 9.85 (s, 1H, OH), 11.20 (s, 1H, NH).

2-(2,4-Dimethoxybenzylidene)hydrazinocarbothioamide (4l): Yield 69%, m.p. 221-223 °C (Pasha et al., 2008), (ethanol/water (2:1)), $C_{10}H_{13}N_3O_2S$. ^{1}H NMR (DMSO-*d*$_6$) δ 3.82 (s, 6H, $2OCH_3$), 6.60 (s, 2H, NH_2), 7.85-8.10 (m, 3H, Ar-H), 8.35 (s, 1H, CH=N), 11.30 (s, 1H, NH).

2-((1*H*-Pyrrol-2-yl)methylidene)hydrazinocarbothioamide (4m): Yield 84%, m.p. 200-201 °C (Yi et al., 2011), (methanol), $C_6H_8N_4S$. ^{1}H NMR (DMSO-*d*$_6$) δ 6.15-7.95 (m, 5H, pyrrole-H, NH_2), 7.90 (s, 1H, CH=N), 11.20 (s, 1H, NH), 11.35 (s, 1H, NH).

2-((1,1'-Biphenyl)-4-ylmethylidene)hydrazinocarbothioamide (4n): Yield 80%, m.p. 202-203 °C (Mendoza-Merono et al., 2010), (ethanol/water (2:1)), $C_{14}H_{13}N_3S$. ^{1}H NMR (DMSO-*d*$_6$) *δ* 7.45-8.25 (m, 12H, Ar-H, NH_2, CH=N), 11.50 (s, 1H, NH). ^{13}C NMR (DMSO-*d*$_6$) *δ* 127.1, 127.3, 128.2, 128.3, 129.4, 133.7, 139.8, 141.7, 142.3, 178.4.

2-(Naphthalen-2-ylmethylidene)hydrazinocarbothioamide (4o): Yield 88%, m.p. 245-246 °C (Yi et al., 2011), (ethanol/water (2:1)), $C_{12}H_{11}N_3S$. ^{1}H NMR (DMSO-*d*$_6$) *δ* 7.10-8.70 (m, 10H, Ar-H, NH_2, CH=N), 11.55 (s, 1H, NH).

2-((1-Nitronaphthalen-2-yl)methylidene)hydrazinocarbothioamide (4p): Yield 77%, m.p. 183-185 °C, (ethyl acetate/ethanol (3:1)). ^{1}H NMR (DMSO-*d*$_6$) *δ* 7.60-8.45 (m, 9H, Ar-H, NH_2, CH=N), 11.70 (s, 1H, NH). Anal. $C_{12}H_{10}N_4O_2S$ (C, H, N).

2-((2-Oxo-2*H*-chromen-6-yl)methylidene)hydrazinocarbothioamide (4q): Yield 71%, m.p. 276-278 °C (Datta and Daniels, 1963), (methanol), $C_{11}H_9N_3O_2S$. ^{1}H NMR (DMSO-*d*$_6$) *δ* 6.55-8.20 (m, 8H, Ar-H, C4-H of chromone, NH_2, CH=N), 11.55 (s, 1H, NH).

2-((10-Chloroanthracen-9-yl)methylidene)hydrazinocarbothioamide (4r): Yield 81%, m.p. 195-197 °C, (ethyl acetate/ethanol (3:1)). ^{1}H NMR (DMSO-*d*$_6$) *δ* 7.70-8.65 (m, 10H, Ar-H), 9.20 (s, 1H, CH=N), 11.85 (s, 1H, NH). Anal. $C_{16}H_{12}ClN_3S$ (C, H, N).

2-(Phenanthren-9-ylmethylidene)hydrazinocarbothioamide (4s): Yield 69%, m.p. 219-220 °C (Ebrahimi et al., 2015), (ethanol/water (2:1)), $C_{16}H_{13}N_3S$. ^{1}H NMR (DMSO-*d*$_6$) *δ* 7.65-8.95 (m, 12H, Ar-H, NH_2, CH=N), 11.55 (s, 1H, NH). ^{13}C NMR (DMSO-*d*$_6$) *δ* 123.3, 123.9, 124.4, 127.4, 127.7, 127.9, 128.0, 128.2, 128.4, 128.7, 129.4, 130.5, 130.7, 131.2, 142.0, 178.4.

2-(Pyren-2-ylmethylidene)hydrazinocarbothioamide (4t): Yield 83%, m.p. 200-202 °C, (ethyl acetate/ethanol (3:1)). ^{1}H NMR (DMSO-*d*$_6$) *δ* 8.05-8.90 (m, 11H, Ar-H, NH_2), 9.25 (s, 1H, CH=N), 11.65 (s, 1H, NH). Anal. $C_{18}H_{13}N_3S$ (C, H, N).

Synthesis of hydrazinothiazolylcoumarin derivatives 5a-t: 3-(Bromoacetyl)coumarin **(3)** (0.107 g, 4 mmol), 2-arylidenehydrazinocarbothioamides **4a-t** (4 mmol) and glacial acetic acid (0.1 mL) were heated in ethanol (10 mL) under microwave irradiation (60 W) at 100 °C for 10 min. The attained solid was filtered and crystallized to give **5a-t**.

3-(2-(2-(2-Bromobenzylidene)hydrazino)-thiazol-4-yl)-2*H*-chromen-2-one (5a): Yield 75%, m.p. 212-213 °C, (ethanol/water (2:1)). ^{1}H NMR (DMSO-*d*$_6$) *δ* 7.30-8.65 (m, 11H, Ar-H, C_5-H of thiazole, C_4-H of chromone, CH=N), 12.50 (s, 1H, NH). ^{13}C NMR (DMSO-*d*$_6$) *δ* 116.3, 119.6, 120.9, 123.1, 125.2, 127.1, 128.6, 129.3, 129.9, 131.4, 132.2, 133.4, 133.6, 138.7, 140.2, 144.5, 152.8, 159.2, 167.9. HRMS: *m/z* (ESI) calcd for $C_{19}H_{11}BrN_3O_2S^-$, $[M-H]^-$: 423.9749; found: 423.9758. Anal. $C_{19}H_{12}BrN_3O_2S$ (C, H, N).

3-(2-(2-(2-Cyanobenzylidene)hydrazino)-thiazol-4-yl)-2*H*-chromen-2-one (5b): Yield 69%, m.p. 219-220 °C, (ethanol/water (2:1)). ^{1}H NMR (DMSO-*d*$_6$) *δ* 7.30-8.80 (m, 11H, Ar-H, C_5-H of thiazole, C_4-H of chromone, CH=N), 12.55 (s, 1H, NH). ^{13}C NMR (DMSO-*d*$_6$) *δ* 112.3, 113.6, 116.1, 120.7, 123.1, 125.2, 127.3, 128.9, 129.7, 129.9, 131.7, 132.1, 132.9, 133.5, 138.2, 143.7, 145.8, 152.6, 161.3, 168.4. HRMS: *m/z* (ESI) calcd for $C_{20}H_{11}N_4O_2S^-$, $[M-H]^-$: 371.0581; found: 371.0593. Anal. $C_{20}H_{12}N_4O_2S$ (C, H, N).

3-(2-(2-(3-Cyanobenzylidene)hydrazino)-thiazol-4-yl)-2*H*-chromen-2-one (5c): Yield 63%, m.p. 224-225 °C, (methanol). ^{1}H NMR (DMSO-*d*$_6$) *δ* 7.30-8.10 (m, 10H, Ar-H), 8.55 (s, 1H, CH=N), 12.40 (s, 1H, NH). HRMS: *m/z* (ESI) calcd for $C_{20}H_{13}N_4O_2S^+$, $[M+H]^+$:

373.0785; found: 373.0766. Anal. $C_{20}H_{12}N_4O_2S$ (C, H, N).

3-(2-(2-(4-(Trifluoromethyl)benzylidene)-hydrazino)thiazol-4-yl)-2*H*-chromen-2-one (5d): Yield 72%, m.p. 189-190 °C, (ethanol/water (2:1)). ^{1}H NMR (DMSO-*d*$_6$) δ 7.30-8.15 (m, 9H, Ar-H, C_5-H of thiazole), 8.30 (s, 1H, C_4-H of chromone), 8.60 (s, 1H, CH=N), 12.45 (s, 1H, NH). ^{13}C NMR (DMSO-*d*$_6$) δ 111.5, 116.3, 119.6, 120.9, 125.2, 126.1, 126.2, 127.4, 129.2, 129.3, 132.2, 138.7, 140.3, 144.5, 152.7, 159.2, 159.3, 167.9. HRMS: *m/z* (ESI) calcd for $C_{20}H_{11}F_3N_3O_2S^-$, $[M-H]^-$: 414.0535; found: 414.0541. Anal. $C_{20}H_{12}F_3N_3O_2S$ (C, H, N).

3-(2-(2-(3-Methylbenzylidene)hydrazino)-thiazol-4-yl)-2*H*-chromen-2-one (5e): Yield 82%, m.p. 190-191 °C, (ethyl acetate/ethanol (3:1)). ^{1}H NMR (DMSO-*d*$_6$) δ 2.30 (s, 3H, CH_3), 7.15-8.05 (m, 9H, Ar-H, C_5-H of thiazole), 8.30 (s, 1H, C_4-H of chromone), 8.52 (s, 1H, CH=N), 12.20 (s, 1H, NH). ^{13}C NMR (DMSO-*d*$_6$) δ 21.4, 111.1, 116.3, 119.6, 120.9, 121.6, 124.1, 125.2, 127.1, 129.2, 129.3, 130.5, 132.1, 138.5, 138.6, 142.3, 144.4, 152.7, 159.2, 168.1. HRMS: *m/z* (ESI) calcd for $C_{20}H_{14}N_3O_2S^-$, $[M-H]^-$: 360.0800; found: 360.0813. Anal. $C_{20}H_{15}N_3O_2S$ (C, H, N).

3-(2-(2-(2,6-Dichlorobenzylidene)hydrazino)thiazol-4-yl)-2*H*-chromen-2-one (5f): Yield 81%, m.p. 230-232 °C, (chloroform). ^{1}H NMR (DMSO-*d*$_6$) δ 7.30-7.90 (m, 8H, Ar-H, C_5-H of thiazole), 8.30 (s, 1H, C_4-H of chromone), 8.60 (s, 1H, CH=N), 12.50 (s, 1H, NH). ^{13}C NMR (DMSO-*d*$_6$) δ 111.7, 116.3, 119.6, 120.9, 125.1, 125.3, 129.3, 130.9, 132.1, 134.0, 136.8, 139.7, 144.4, 152.8, 159.2, 159.3, 167.9. HRMS: *m/z* (ESI) calcd for $C_{19}H_{12}Cl_2N_3O_2S^+$, $[M+H]^+$: 416.0034; found: 416.0030. Anal. $C_{19}H_{11}Cl_2N_3O_2S$ (C, H, N).

3-(2-(2-(2-Chloro-6-fluorobenzylidene)hydrazino)thiazol-4-yl)-2*H*-chromen-2-one (5g): Yield 69%, m.p. 195-196 °C, (ethanol/water (2:1)). ^{1}H NMR (DMSO-*d*$_6$) δ 7.25-7.90 (m, 8H, Ar-H, C_5-H of thiazole), 8.25 (s, 1H, C_4-H of chromone), 8.65 (s, 1H, CH=N), 12.50 (s, 1H, NH). ^{13}C NMR (DMSO-*d*$_6$) δ 111.7, 115.9, 116.1, 119.6, 120.8, 120.9, 125.2, 126.7, 126.8, 129.3, 133.4, 134.7, 138.7, 144.4, 152.8, 159.2, 159.3, 161.9, 167.9. HRMS: *m/z* (ESI) calcd for $C_{19}H_{12}ClFN_3O_2S^+$, $[M+H]^+$: 400.0328; found: 400.0314. Anal. $C_{19}H_{11}ClFN_3O_2S$ (C, H, N).

3-(2-(2-(2-Chloro-5-nitrobenzylidene)hydrazino)thiazol-4-yl)-2*H*-chromen-2-one (5h): Yield 74%, m.p. 176-177 °C, (ethanol/water (2:1)). ^{1}H NMR (DMSO-*d*$_6$) δ 7.30-8.65 (m, 10H, Ar-H, C_5-H of thiazole, C_4-H of chromone, CH=N), 12.70 (s, 1H, NH). ^{13}C NMR (DMSO-*d*$_6$) δ 112.3, 120.9, 123.1, 125.4, 125.7, 126.9, 127.2, 128.4, 129.3, 129.9, 133.7, 138.1, 141.0, 142.8, 145.9, 146.2, 151.3, 161.6, 169.2. HRMS: *m/z* (ESI) calcd for $C_{19}H_{12}ClN_4O_4S^+$, $[M+H]^+$: 427.0246; found: 427.0267. Anal. $C_{19}H_{11}ClN_4O_4S$ (C, H, N).

3-(2-(2-(3-Bromo-4-hydroxybenzylidene)-hydrazino)thiazol-4-yl)-2*H*-chromen-2-one (5i): Yield 80 %, m.p. 182-184 °C, (ethyl acetate/ethanol (3:1)). ^{1}H NMR (DMSO-*d*$_6$) δ 7.00-8.85 (m, 10H, Ar-H, C_5-H of thiazole, C_4-H of chromone, CH=N), 10.85 (s, 1H, OH), 12.05 (s, 1H, NH). HRMS: *m/z* (ESI) calcd for $C_{19}H_{11}BrN_3O_3S^-$, $[M-H]^-$: 439.9685; found: 439.9698. Anal. $C_{19}H_{12}BrN_3O_3S$ (C, H, N).

3-(2-(2-(2-Hydroxy-5-methylbenzylidene)-hydrazino)thiazol-4-yl)-2*H*-chromen-2-one (5j): Yield 84%, m.p. 206-207 °C, (ethyl acetate/ethanol (3:1)). ^{1}H NMR (DMSO-*d*$_6$) δ 2.20 (s, 3H, CH_3), 6.80-7.90 (m, 8H, Ar-H, C_5-H of thiazole), 8.30 (s, 1H, C_4-H of chromone), 8.55 (s, 1H, CH=N), 9.80 (s, 1H, OH), 12.15 (s, 1H, NH). ^{13}C NMR (DMSO-*d*$_6$) δ 20.6, 110.8, 116.3, 116.5, 119.6, 120.1, 120.9, 125.2, 126.7, 128.4, 129.3, 131.8, 132.1, 138.6, 140.6, 144.6, 152.8, 154.4, 159.2, 167.8. HRMS: *m/z* (ESI) calcd for

$C_{20}H_{14}N_3O_3S^-$, [M-H]$^-$: 376.0781; found: 376.0771. Anal. $C_{20}H_{15}N_3O_3S$ (C, H, N).

3-(2-(2-(4-Hydroxy-3-methylbenzylidene)-hydrazino)thiazol-4-yl)-2*H*-chromen-2-one (5k): Yield 71%, m.p. 193-194 °C, (ethanol/water (2:1)). ^{1}H NMR (DMSO-*d*$_6$) *δ* 2.15 (s, 3H, CH_3), 6.80 (s, 1H, C_5-H of thiazole), 7.25-7.95 (m, 8H, Ar-H, C_4-H of chromone), 8.50 (s, 1H, CH=N), 9.75 (s, 1H, OH), 11.90 (s, 1H, NH). HRMS: *m/z* (ESI) calcd for $C_{20}H_{14}N_3O_3S^-$, [M-H]$^-$: 376.0781; found: 376.0765. Anal. $C_{20}H_{15}N_3O_3S$ (C, H, N).

3-(2-(2-(2,4-Dimethoxybenzylidene)-hydrazino)thiazol-4-yl)-2*H*-chromen-2-one (5l): Yield 79%, m.p. 219-220 °C, (chloroform). ^{1}H NMR (DMSO-*d*$_6$) *δ* 3.80 (s, 3H, OCH_3), 3.86 (s, 3H, OCH_3), 6.65-8.55 (m, 10H, Ar-H, C_5-H of thiazole, C_4-H of chromone, CH=N), 11.90 (s, 1H, NH). ^{13}C NMR (DMSO-*d*$_6$) *δ* 56.1, 56.2, 102.3, 106.3, 111.3, 115.6, 120.6, 121.8, 125.9, 126.6, 128.2, 129.6, 132.3, 136.7, 144.1, 146.4, 151.3, 159.6, 161.3, 163.5, 169.1. HRMS: *m/z* (ESI) calcd for $C_{21}H_{18}N_3O_4S^+$, [M+H]$^+$: 408.1037; found: 408.1025. Anal. $C_{21}H_{17}N_3O_4S$ (C, H, N).

3-(2-(2-((1*H*-Pyrrol-2-yl)methylidene)hydrazino)thiazol-4-yl)-2*H*-chromen-2-one (5m): Yield 62%, m.p. 167-168 °C, (chloroform). ^{1}H NMR (DMSO-*d*$_6$) *δ* 6.10-6.90 (m, 4H, pyrrole-H, C_5-H of thiazole), 7.30-7.95 (m, 5H, Ar-H, C_4-H of chromone), 8.55 (s, 1H, CH=N), 11.30 (s, 1H, NH), 11.85 (s, 1H, NH). ^{13}C NMR (DMSO-*d*$_6$) *δ* 111.3, 113.7, 116.6, 120.3, 120.9, 125.1, 125.6, 128.1, 128.6, 129.7, 133.1, 139.4, 145.2, 146.3, 155.4, 162.1, 170.9. HRMS: *m/z* (ESI) calcd for $C_{17}H_{11}N_4O_2S^-$, [M-H]$^-$: 335.0610; found: 335.0619. Anal. $C_{17}H_{12}N_4O_2S$ (C, H, N).

3-(2-(2-((1,1'-Biphenyl)-4-ylmethylidene)-hydrazino)thiazol-4-yl)-2*H*-chromen-2-one (5n): Yield 77%, m.p. 198-200 °C, (ethyl acetate/ethanol (3:1)). ^{1}H NMR (DMSO-*d*$_6$) *δ* 7.30-8.65 (m, 16H, Ar-H, C_5-H of thiazole, C_4-H of chromone, CH=N), 12.25 (s, 1H, NH). ^{13}C NMR (DMSO-*d*$_6$) *δ* 111.2, 116.4, 119.6, 121.0, 125.2, 127.1, 127.4, 127.5, 128.3, 129.3, 129.5, 132.2, 133.8, 138.7, 139.8, 141.3, 141.8, 144.5, 152.8, 159.3, 168.2. HRMS: *m/z* (ESI) calcd for $C_{25}H_{16}N_3O_2S^-$, [M-H]$^-$: 422.0955; found: 422.0959. Anal. $C_{25}H_{17}N_3O_2S$ (C, H, N).

3-(2-(2-(Naphthalen-2-ylmethylidene)hydrazino)thiazol-4-yl)-2*H*-chromen-2-one (5o): Yield 79%, m.p. 225-227 °C, (ethyl acetate/ethanol (3:1)). ^{1}H NMR (DMSO-*d*$_6$) *δ* 7.30-8.60 (m, 14H, Ar-H, C_5-H of thiazole, C_4-H of chromone, CH=N), 12.30 (s, 1H, NH). HRMS: *m/z* (ESI) calcd for $C_{23}H_{14}N_3O_2S^-$, [M-H]$^-$: 396.0812; found: 396.0795. Anal. $C_{23}H_{15}N_3O_2S$ (C, H, N).

3-(2-(2-((1-Nitronaphthalen-2-yl)methylidene)hydrazino)thiazol-4-yl)-2*H*-chromen-2-one (5p): Yield 63%. m.p. 211-213 °C, (chloroform). ^{1}H NMR (DMSO-*d*$_6$) *δ* 7.35-8.25 (m, 12H, Ar-H, C_5-H of thiazole, C_4-H of chromone), 8.55 (s, 1H, CH=N), 12.75 (s, 1H, NH). ^{13}C NMR (DMSO-*d*$_6$) *δ* 113.2, 115.9, 121.1, 123.6, 124.2, 125.1, 125.7, 126.3, 127.3, 127.6, 128.4, 128.9, 129.5, 129.8, 135.2, 137.4, 142.9, 144.6, 145.9, 147.2, 154.3, 162.2, 171.7. HRMS: *m/z* (ESI) calcd for $C_{23}H_{13}N_4O_4S^-$, [M-H]$^-$: 441.0663; found: 441.0660. Anal. $C_{23}H_{14}N_4O_4S$ (C, H, N).

6-((2-(4-(2-Oxo-2*H*-chromen-3-yl)thiazol-2-yl)hydrazono)methyl)-2*H*-chromen-2-one (5q): Yield 76%, m.p. 181-183 °C, (ethanol/water (2:1)). ^{1}H NMR (DMSO-*d*$_6$) *δ* 6.50 (d, 1H, C_3-H of chromone), 7.30-8.15 (m, 10H, Ar-H, C_5-H of thiazole, C_4-H of two chromone moieties), 8.55 (s, 1H, CH=N), 12.25 (s, 1H, NH). ^{13}C NMR (DMSO-*d*$_6$) *δ* 111.2, 116.3, 117.2, 117.5, 119.5, 119.6, 120.9, 125.2, 126.7, 129.2, 129.7, 131.2, 132.2, 138.6, 140.6, 144.5, 151.9, 152.7, 154.3, 159.2, 160.1, 168.0. HRMS: *m/z* (ESI) calcd for $C_{22}H_{12}N_3O_4S^-$, [M-H]$^-$: 414.0560; found: 414.0565. Anal. $C_{22}H_{13}N_3O_4S$ (C, H, N).

EXCLI Journal 2017;16:1114-1131 – ISSN 1611-2156
Received: February 10, 2017, accepted: July 31, 2017, published: August 30, 2017

3-(2-(2-((10-Chloroanthracen-9-yl)-methylidene)hydrazino)thiazol-4-yl)-2*H*-chromen-2-one (5r): Yield 86%, m.p. 238-240 °C, (ethanol/water (2:1)). ^{1}H NMR (DMSO-d_6) δ 7.20-8.75 (m, 15H, Ar-H, C_5-H of thiazole, C_4-H of chromone, CH=N), 12.50 (s, 1H, NH). ^{13}C NMR (DMSO-d_6) δ 111.3, 116.4, 120.4, 122.5, 125.1, 125.2, 125.9, 126.7, 127.8, 128.4, 128.8, 129.3, 130.1, 132.5, 134.0, 138.8, 140.1, 142.3, 152.0, 164.2, 168.0. HRMS: *m/z* (ESI) calcd for $C_{27}H_{15}ClN_3O_2S^-$, $[M-H]^-$: 480.0574; found: 480.0574. Anal. $C_{27}H_{16}ClN_3O_2S$ (C, H, N).

3-(2-(2-(Phenanthren-9-ylmethylidene)-hydrazino)thiazol-4-yl)-2*H*-chromen-2-one (5s): Yield 87%, m.p. 245-247 °C, (chloroform). ^{1}H NMR (DMSO-d_6) δ 7.30-8.20 (m, 11H, Ar-H, C_5-H of thiazole, C_4-H of chromone, CH=N), 8.55-9.10 (m, 5H, Ar-H), 12.45 (s, 1H, NH). HRMS: *m/z* (ESI) calcd for $C_{27}H_{16}N_3O_2S^-$, $[M-H]^-$: 446.0941; found: 446.0960. Anal. $C_{27}H_{17}N_3O_2S$ (C, H, N).

3-(2-(2-(Pyren-2-ylmethylidene)hydrazino) thiazol-4-yl)-2*H*-chromen-2-one (5t): Yield 89%, m.p. 237-239 °C, (ethanol/water (2:1)). ^{1}H NMR (DMSO-d_6) δ 7.35-9.00 (m, 16H, Ar-H, C_5-H of thiazole, C_4-H of chromone, CH=N), 12.50 (s, 1H, NH). HRMS: *m/z* (ESI) calcd for $C_{29}H_{16}N_3O_2S^-$, $[M-H]^-$: 470.0975; found: 470.0979. Anal. $C_{29}H_{17}N_3O_2S$ (C, H, N).

Biology

Detailed biological screening methods are provided in the supplementary information.

In vitro antitumor assay

The new analogs were tested for *in vitro* antitumor efficacy adopting the reported procedure (Mosmann, 1983; Denizot and Lang, 1986; Gerlier and Thomasset, 1986).

In vivo antitumor assay

In vivo antitumor assessment of **5f, 5h, 5m** and **5r** was performed according to the literature method (Oberling and Guerin, 1954; Sheeja et al., 1997; Clarkson and Burchenal, 1965).

In vitro cytotoxicity testing

In vitro cytotoxic activity of **5f, 5h, 5m** and **5r** was evaluated in accord to the reported method (Mosmann, 1983; Denizot and Lang, 1986; Gerlier and Thomasset, 1986).

RESULTS AND DISCUSSION

Chemistry

3-(Bromoacetyl)coumarin **(3)** was synthesized *via* a two step procedure (Figure 2). First, cyclocondensation of salicylaldehyde **(1)** and ethyl acetoacetate under microwave irradiation utilizing piperidine as a catalyst to give the 3-acetylcoumarin **(2)** (Valizadeh et al., 2007). Second, bromination of compound **2** in chloroform to yield the bromoketone **3** in 63% yield (Siddiqui et al., 2009) (Figure 2). The 2-arylidenehydrazinocarbothioamides **4a-t** were synthesized through condensation of the aromatic aldehydes and thiosemicarbazide in ethanol under microwave irradiation (Figure 3). Microwave irradiation of **4a-t** and bromoketone **3** in ethanol, followed by addition of ammonium hydroxide 5%, furnished the desired thiazolylcoumarin hybrids **5a-t** in moderate to good yields (62-89%) (Figure 3).

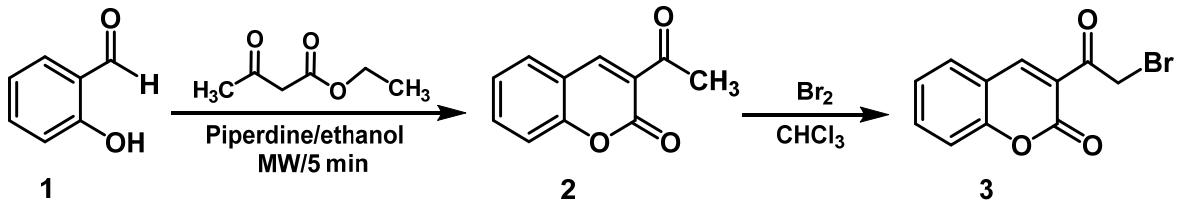

Figure 2: Synthesis of 3-(bromoacetyl)coumarin **(3)**

EXCLI Journal 2017;16:1114-1131 – ISSN 1611-2156
Received: February 10, 2017, accepted: July 31, 2017, published: August 30, 2017

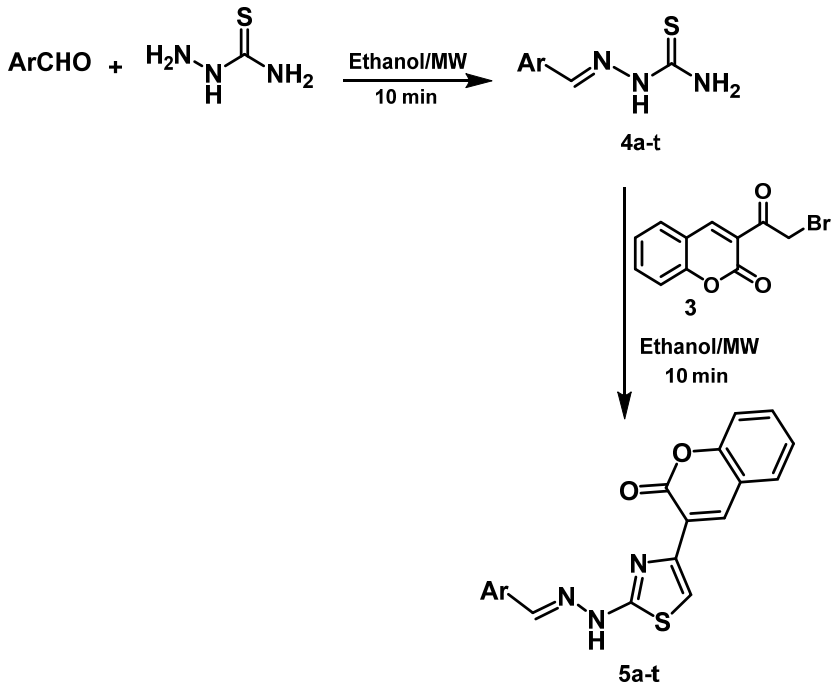

Comp. No.	Ar	Comp. No.	Ar	Comp. No.	Ar	Comp. No.	Ar
a		b		c		d	
e		f		g		h	
i		j		k		l	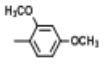
m		n		o		p	
q		r		s		t	

Figure 3: Synthesis of thiazolylcoumarin hybrids **5a-t**

Biological screening

In vitro antitumor screening

In vitro antitumor screening of compounds **5a-t** was carried out on cervical (Hela) and kidney fibroblast (COS-7) cancer cell lines in accord to MTT assay (Mosmann, 1983; Denizot and Lang, 1986; Gerlier and Thomasset, 1986) and utilizing doxorubicin as a standard drug. The concentrations of the compounds that cause 50% inhibition of cell viability (IC_{50}, μM) were calculated. Compounds **5f, 5h, 5m** and **5r** exhibited remarkable activity against Hela cell line. In addition, **5h** and **5r** displayed outstanding efficacy toward COS-7 cell line (Table 1). The rest of the tested compounds displayed weaker efficacy.

Structure-activity relationship

Compound **5f** incorporating 2,6-dichlorophenyl moiety displayed prominent antitumor efficacy toward Hela cell line and it represents the basic framework for further structural modifications. Replacing this moiety with 2-chloro-6-fluorophenyl counterpart

EXCLI Journal 2017;16:1114-1131 – ISSN 1611-2156
Received: February 10, 2017, accepted: July 31, 2017, published: August 30, 2017

Table 1: *In vitro* antitumor activity of **5a-t** toward Hela and COS-7 cancer cell lines

Comp. No.	IC_{50} (µM)		Comp. No.	IC_{50} (µM)	
	Hela	**COS-7**		**Hela**	**COS-7**
5a	>50	>50	**5l**	>50	>50
5b	>50	>50	**5m**	**6.25**	**12.50**
5c	>50	>50	**5n**	>50	>50
5d	>50	>50	**5o**	>50	>50
5e	>50	>50	**5p**	>50	>50
5f	**1.90**	>50	**5q**	>50	>50
5g	>50	>50	**5r**	**1.29**	**1.66**
5h	**1.42**	**1.96**	**5s**	>50	>50
5i	>50	>50	**5t**	>50	>50
5j	>50	>50	**Doxorubicin**	2.05	3.04
5k	>50	>50	--------	--------	--------

Bold values refer to the good results

abolished the activity against the same cell line (compound **5g**), whereas its replacement with 2-chloro-5-nitrophenyl counterpart led to increased efficacy toward the same cell line and a tremendous improvement in the activity toward COS-7 cell line (compound **5h**). Incorporation of pyrrol-2-yl moiety into the thiazolylcoumarin resulted in considerable efficiency toward Hela and COS-7 cell lines which might be attributed to additional interaction with the target receptor (compound **5m**). 10-Chloroanthracen-9-yl moiety was proved to exhibit the optimum hydrophobic binding affinity and displayed the most potent antitumor efficacy against both cell lines (compound **5r**).

In vivo antitumor screening

Results of *in vivo* antitumor screening of compounds **5f**, **5h**, **5m** and **5r** (showing the highest *in vitro* antitumor activity) against EAC cells in mice are listed in Tables 2-4. The % increase in lifespan of EAC inoculated mice (%ILS), the decrease in viable tumor cell count and the retrieval of normal blood profile are three substantial measures used for estimation of antitumor efficacy of the selected compounds and 5-fluorouracil (5-FU) (standard agent) (Oberling and Guerin, 1954; Sheeja et al., 1997; Clarkson and Burchenal, 1965). The mean survival time (MST) of each group was rated and %ILS of mice inoculated with EAC cells was determined adopting the equation: %ILS = [(MST of treated group/ MST of positive control group)-1] x 100, where MST = days of the mouse in a group/total no. of mice. Compound **5r** displayed prominent increase in lifespan of mice (Table 2). Also, this compound produced considerable decrease in viable tumor cell count (Table 3). Regarding the effect on blood profile, compound **5r** showed higher Hb and RBC levels and lower WBC count than 5-FU (Table 4).

Table 2: Effect of **5f, 5h, 5m** and **5r** on mean survival time and % increase in lifespan of mice inoculated with EAC cells

Group	Mean survival time (day)	% Increase in lifespan
Normal	nd[a]	nd[a]
EAC only	14.5	nd[a]
5f	41.0	182.7
5h	39.3	171.0
5m	37.0	155.2
5r	**45.5**	**213.8**
5-Fluorouracil	49.0	237.9

[a] nd: not determined.
Bold values refer to the good results.

Table 3: Effect of **5f, 5h, 5m** and **5r** on tumor volume and viable tumor cell count of mice inoculated with EAC cells

Group	Tumor volume (mL)	Viable tumor cell count/100 µL
Normal	nd[a]	nd[a]
EAC only	9.85	$83.20x10^6$
5f	2.62	$25.83x10^6$
5h	3.12	$32.57x10^6$
5m	3.85	$40.52x10^6$
5r	**2.11**	**$21.94x10^6$**
5-Fluorouracil	1.60	$20.17x10^6$

[a] nd: not determined.
Bold values refer to the good results.

EXCLI Journal 2017;16:1114-1131 – ISSN 1611-2156
Received: February 10, 2017, accepted: July 31, 2017, published: August 30, 2017

Table 4: Effect of **5f, 5h, 5m** and **5r** on blood profile of mice inoculated with EAC cells

Group	Hb (g/dl)	RBCs Count 10^6/mm^3	WBCs Count 10^3/mm^3
Normal	13.73	5.84	5.99
EAC only	8.15	3.69	23.96
5f	12.92	5.14	8.41
5h	11.97	4.92	9.25
5m	11.43	4.39	9.61
5r	**13.10**	**5.55**	**7.45**
5-Fluorouracil	12.96	5.21	8.86

Bold values refer to the good results.

In vitro cytotoxicity testing

The effective antitumor compounds, **5f**, **5h**, **5m** and **5r** were further assessed for *in vitro* cytotoxicity toward human normal lung fibroblast (W138) cell line (Mosmann, 1983; Denizot and Lang, 1986; Gerlier and Thomasset, 1986). IC_{50} values (µM) of the tested compounds and 5-FU (reference cytotoxic agent) were calculated. Results (Table 5) revealed that the four tested compounds are less cytotoxic than 5-FU. Comparing the IC_{50} values of **5h**, **5m** and **5r** on the tested normal cell line (19.75-29.47 µM) with those on the tested cancer cell lines (1.29-12.50 µM), we can conclude that the three compounds are more selective cytotoxic agents toward cancer cells than normal cells. In addition, **5f** was found to be more selective toward Hela cancer cell line (IC_{50} = 1.90 µM) than W138 normal cell line (IC_{50} = 36.21 µM).

Table 5: *In vitro* cytotoxic activity of **5f, 5h, 5m** and **5r** toward W138 normal cell line

Comp. No.	IC_{50} (µM)
5f	36.21
5h	19.75
5m	29.47
5r	24.32
5-Fluorouracil	5.73

3D Pharmacophore elucidation

A pharmacophore is a set of common structural features shared by a group of compounds that interacts with the complementary sites on a specific target leading to biological activity (Rodolpho and Andrade, 2013). Based on this assumption, analysis of the molecular recognitions in the biological target interacting with the lead compound will enable the design of more potent analogs.

LigandScout software allows accurate virtual screening based on 3D pharmacophore models, and it is utilized to produce a pharmacophore for trichostatin A (Wolber and Langer, 2005). The model (Figure 4) was generated by overlaying the pharmacophoric features of HDAC8 domain complexed with trichostatin A (PDB ID: 1T64) (PDB; http://www.rcsb.org/pdb/home/home.do).

The pharmacophore created by LigandScout revealed the presence of one hydrogen bond acceptor site (red arrow) embedded between five hydrophobic regions represented by yellow spheres which conveys the tremendous contribution of hydrophobic interactions with the receptor. Moreover, ZBG represented by a blue conical shape, was oriented at the terminal of the hydrophobic regions and is proposed to be an essential feature in the presented pharmacophore. The four active antitumor compounds in this study, **5f**, **5h**, **5m** and **5r** were subjected to a pharmacophore-based virtual screening against the target pharmacophore of trichostatin A. The matching pharmacophoric features between the active compounds and trichostatin A are identified in Table 6. All the active compounds attained a ZBG, a hydrogen bond acceptor site and at least two sites for hydrophobic interactions matching the orientation exhibited by the target pharmacophore. In addition, a relative pharmacophore score illustrated in Table 6 was calculated for each compound. Compounds **5f** and **5r** exhibited the highest relative pharmacophore score of 0.76 and 0.81, respectively. Figures 5A and 6A illustrate the 3D alignments of **5f** and **5r**, respectively with the pharmacophore model. 2D Mappings of the pharmacophore model with **5f** and **5r** are shown in Figures 5B and 6B, respectively. The proposed pharmacophore of HDAC8 revealed that hydrophobic forces represent the major contributing interaction with the compounds, accordingly, LeadIT program was utilized to examine the

EXCLI Journal 2017;16:1114-1131 – ISSN 1611-2156
Received: February 10, 2017, accepted: July 31, 2017, published: August 30, 2017

hydrophobic interaction of the active analogs with the target receptor (Stahl and Rarey, 2001). The lipophilic area of each compound exposed toward HDAC8 domain was given a score (Table 6). Compounds **5f** and **5r** attained the highest lipophilic area score of -14.12 and -14.65, respectively. 2D Interactions of **5f** and **5r** with HDAC8 domain are presented in Figures 7 and 8, respectively.

In silico studies

Computational chemists follow different approaches for estimation of molecular diversity. Drug-likeness is a qualitative notion used to study how a particular substance is "drug-like". So, computer softwares were utilized for predicting the drug-likeness of the new drugs (Ursu et al., 2011). The most active compounds, **5f**, **5h**, **5m** and **5r** were studied for the expectation of Lipinski's rule (Lipinski et al., 2001) along with other molecular properties.

Table 6: Results of pharmacophore analysis of **5f**, **5h**, **5m** and **5r**

Comp. No.	Matching Features	Relative Pharmacophore Score	Lipophilic Area Score
5f		**0.76**	**-14.12**
5h		0.56	-13.71
5m		0.54	-12.31
5r		**0.81**	**-14.65**
Trichostatin A		1.00	-14.71

: Hydrophobic region; : Zinc binding group; : Hydrogen acceptor

Bold values refer to the good results.

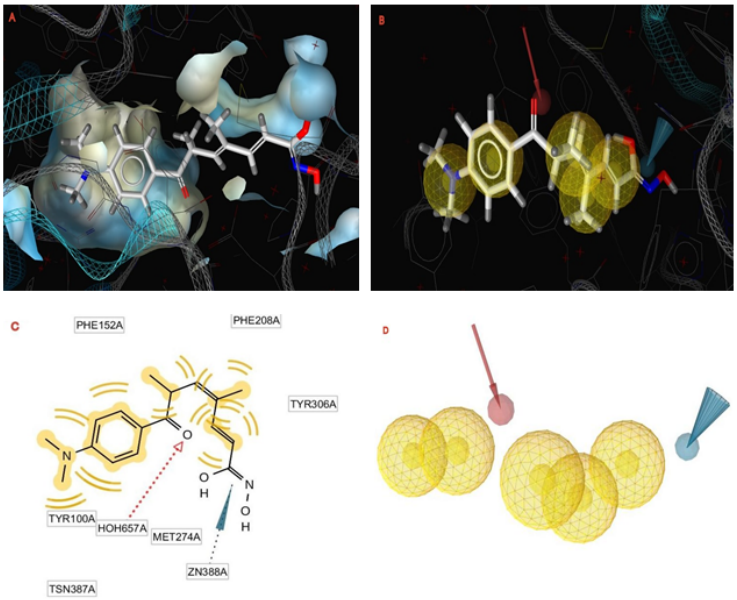

Figure 4: A. LigandScout 3D proposed docking pose for trichostatin A in HDAC8 domain (PDB ID: 1T64). **B**. 3D Pharmacophore of trichostatin A (in ball and stick presentation); The pharmacophore color coding is red for hydrogen acceptor, yellow for hydrophobic regions, and blue for zinc binding group. **C**. 2D Representation of the pharmacophoric features of trichostatin A. **D**. The 3D pharmacophore model for HDAC8 domain (PDB ID: 1T64). The pharmacophore color coding is red for hydrogen acceptor, yellow for hydrophobic regions, and blue for zinc binding group

EXCLI Journal 2017;16:1114-1131 – ISSN 1611-2156
Received: February 10, 2017, accepted: July 31, 2017, published: August 30, 2017

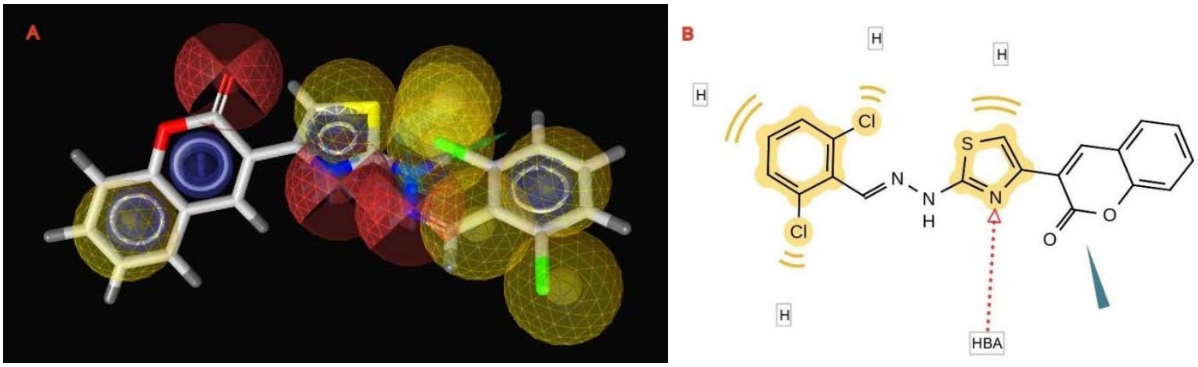

Figure 5: The 3D and 2D alignments of **5f** with HDAC8 pharmacophore model. **A**. 3D Alignment of **5f** with HDAC8 pharmacophore model. The pharmacophore color coding is red for hydrogen acceptors, yellow for hydrophobic regions and blue for zinc binding groups. **B**. 2D Representation of structural features of **5f** that can be aligned with the pharmacophore hypothesis. HBA; hydrogen bond acceptor and H; hydrophobic center

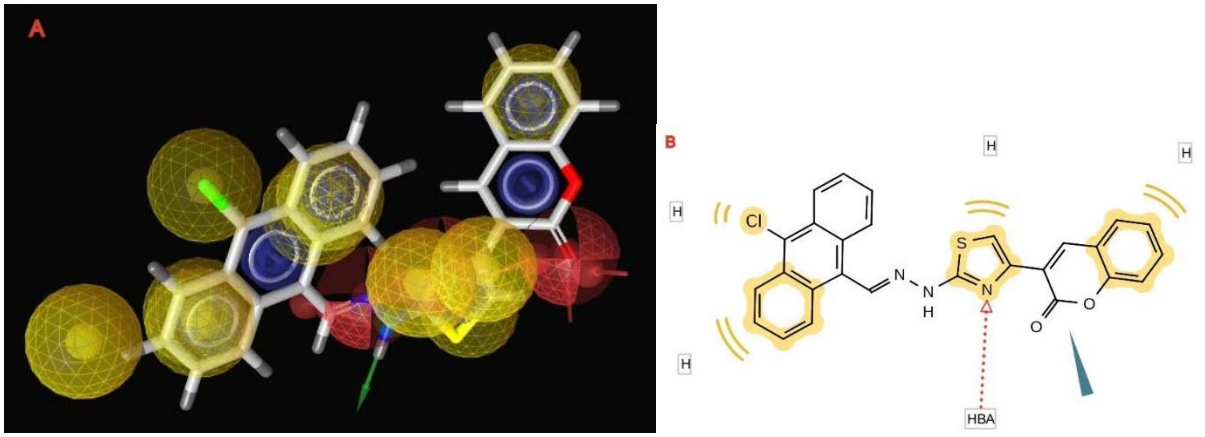

Figure 6: The 3D and 2D alignments of **5r** with HDAC8 pharmacophore model. **A**. 3D Alignment of **5r** with HDAC8 pharmacophore model. The pharmacophore color coding is red for hydrogen acceptors, yellow for hydrophobic regions and blue for zinc binding groups. **B**. 2D Representation of structural features of **5r** that can be aligned with the pharmacophore hypothesis. HBA; hydrogen bond acceptor and H; hydrophobic center

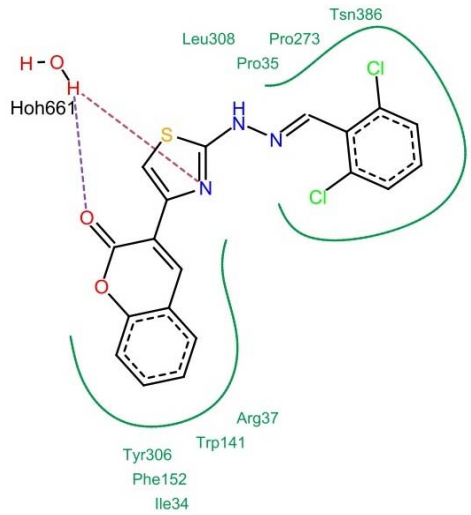

Figure 7: 2D Interaction of **5f** with HDAC8 domain. Hydrogen bonds are shown by dashed lines. Green solid lines represent hydrophobic interactions

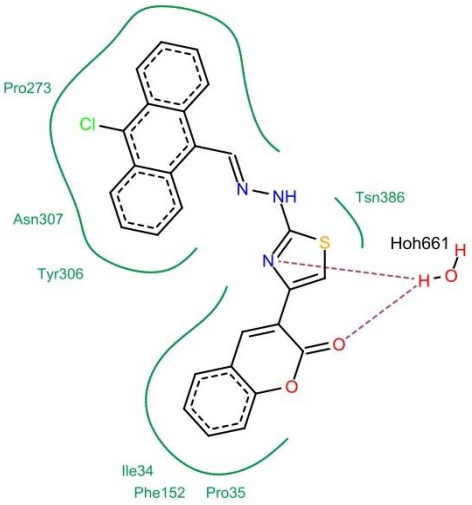

Figure 8: 2D Interaction of **5r** with HDAC8 domain. Hydrogen bonds are shown by dashed lines. Green solid lines represent hydrophobic interactions

EXCLI Journal 2017;16:1114-1131 – ISSN 1611-2156
Received: February 10, 2017, accepted: July 31, 2017, published: August 30, 2017

Molinspiration calculations

Lipinski's rule is related to drug absorption (Lipinski et al., 2001). Also, topological polar surface area (TPSA) and number of rotatable bonds (Nrotb) influence oral absorption of drugs (Veber et al., 2002).

TPSA, Nrotb, and the parameters of Lipinski's rule for the effective analogs, **5f**, **5h**, **5m** and **5r** were evaluated using molinspiration software.

Results illustrated that all examined analogs have zero or one violation of Lipinski's rule, as well as TPSA values and Nrotb under the acceptable norms; therefore, they are anticipated to be well absorbed (Table 7).

Drug-likeness

Osiris software (Jarrahpour et al., 2011) was applied for studying the toxicity hazards (mutagenicity, tumorigenicity, irritation & reproductive effects) and drug-likeness of the analyzed compounds. Results revealed that all the analyzed analogs are expected to have no toxicity hazards. It is well established that molecules containing fragments which are extremely available in commercial drugs, have positive drug-likeness values. Results listed in Table 7 showed that **5f**, **5m** and **5r** have positive drug-likeness values, and they are expected to have fragments which are available in commercial drugs.

CONCLUSION

The recent study led to the development of new efficient antitumor thiazolylcoumarin derivatives. Compounds **5f**, **5h**, **5m** and **5r** are the most active antitumor analogs toward Hela cell line; in addition, **5h** and **5r** displayed eminent activity toward COS-7 cell line. Moreover, **5r** displayed the highest *in vivo* activity. Furthermore, the four active analogs were proved to be less cytotoxic than 5-FU on W138 normal cells; therefore, they might be used as potent antitumor agents with low toxicity toward normal cells. Further mechanistic and kinetic investigations concerning the HDACs inhibitory activity of these active compounds will shed light on possible structural modifications desired to obtain new more active antitumor agents.

Acknowledgments

The authors extend their appreciation to Professor Binghe Wang, Georgia State University, USA, for offering the facilities needed for performing spectral analysis and *in vitro* antitumor testing. Thanks to Mr. Ahmed Abbas, Faculty of Pharmacy, Mansoura University, Egypt, for assessment of *in vivo* antitumor and *in vitro* cytotoxic activities.

Table 7: TPSA, Nrotb, calculated Lipinski's rule and drug-likeness of **5f, 5h, 5m** and **5r**

Comp. No.	Molecular properties							Drug-likeness
	TPSA	Nrotb	miLogP	nOH-NH	nO-N	M. wt.	No. of violations	
5f	67.49	4	5.22	1	5	416.29	1	6.17
5h	113.32	5	4.53	1	8	426.84	0	-1.13
5m	83.28	4	3.12	2	6	336.38	0	5.43
5r	67.49	4	6.86	1	5	481.96	1	5.23

REFERENCES

Abdul Rahman FS, Yusufzai SK, Osman H, Mohamad D. Synthesis, characterisation and cytotoxicity activity of thiazole substitution of coumarin derivatives (Characterisation of coumarin derivatives). J Phys Sci. 2016;27:77-87.

Abouzeid LA, El-Subbagh HI. DNA binding of ethyl 2-substituted aminothiazole-4-carboxylate analogues: A molecular modeling approach to predict their antitumor activity. Future J Pharm Sci. 2015;1:1-7.

Amin KM, Abou-Seri SM, Awadallah FM, Eissa AM, Hassan GS, Abdulla MM. Synthesis and anticancer activity of some 8-substituted-7-methoxy-2*H*-chromen-2-one derivatives toward hepatocellular carcinoma HepG2 cells. Eur J Med Chem. 2015;90:221-31.

Bagi CM. Cancer cell metastasis session. J Musculoskel Neuron Interact. 2002;2:579-80.

Bernstein J, Yale HL, Losee K, Holsing M, Martins J, Lott WA. The chemotherapy of experimental tuberculosis. 111. The synthesis of thiosemicarbazones and related compounds. J Am Chem Soc. 1951;73:906-12.

Bowers AA, Greshock TJ, West N, Estiu G, Schreiber SL, Wiest O, Williams RM, Bradner JE. Synthesis and conformation-activity relationships of the peptide isosteres of FK228 and largazole. J Am Chem Soc. 2009a;131:2900-5.

Bowers AA, West N, Newkirk TL, Troutman-Yougman AE, Schreiber SL, Wiest O, et al. Synthesis and histone deacetylase inhibitory activity of largazole analogs: Alteration of the zinc-binding domain and macrocyclic scaffold. Org Lett. 2009b;11:1301-4.

Chen K, Xu L, Wiest O. Computational exploration of zinc binding groups for HDAC inhibition. J Org Chem. 2013;78:5051-5.

Clarkson BD, Burchenal JH. Preliminary screening of antineoplastic drugs. Prog Clin Cancer. 1965;1:625-9.

Coxon GD, Craig D, Corrales RM, Vialla E, Gannoun-Zaki L, Kremer L. Synthesis, antitubercular activity and mechanism of resistance of highly effective thiacetazone analogues. PLoS One. 2013;8:e53162, https://doi.org/10.1371/journal.pone.0053162.

Datta AD, Daniels TC. Antitubercular activity of some aromatic aldehyde and ketone derivatives. J Pharm Sci. 1963;52:905-6.

Day JA, Cohen SM. Investigating the selectivity of metalloenzyme inhibitors. J Med Chem. 2013;56:7997-8007.

Denizot F, Lang R. Rapid colorimetric assay for cell growth and survival. Modifications to the tetrazolium dye procedure giving improved sensitivity and reliability. J Immunol Methods. 1986;89:271-7.

Di Micco S, Chini M G, Terracciano S, Bruno I, Riccio R, Bifulco G. Structural basis for the design and synthesis of selective HDAC inhibitors. Bioorg Med Chem. 2013;21:3795-807.

Ebrahimi HP, Hadi JS, Alsalim TA, Ghali TS, Bolandnazar Z. A novel series of thiosemicarbazone drugs: From synthesis to structure. Spectrochim. Acta Mol Biomol Spectrosc. 2015;137:1067-77.

Emami S, Dadashpour S. Current developments of coumarin based anti-cancer agents in medicinal chemistry. Eur J Med Chem. 2015;102:611-30.

Falkenberg KJ, Johnstone RW. Histone deacetylases and their inhibitors in cancer, neurological diseases and immune disorders. Nat Rev Drug Discov. 2014;13:673-91.

Feng T, Wang H, Su H, Lu H, Yu L, Zhang X, et al. Novel *N*-hydroxyfurylacrylamide-based histone deacetylase (HDAC) inhibitors with branched CAP group (Part 2). Bioorg Med Chem. 2013;21:5339-54.

Ganina OG, Daras E, Bourgarel-Rey V, Peyrot V, Andresyuk AN, Finet JP, et al. Synthesis and biological evaluation of polymethoxylated 4-heteroaryl coumarins as tubulin assembly inhibitor. Bioorg Med Chem. 2008;16:8806-12.

Garazd Y, Garazd M, Lesyk R. Synthesis and evaluation of anticancer activity of 6-pyrazolinylcoumarin derivatives. Saudi Pharm J. 2017;25:214-23.

Gerlier D, Thomasset T. Use of MTT colorimetric assay to measure cell activation. J Immunol Methods. 1986; 94:57-63.

Goel R, Luxami V, Paul K. Synthesis, *in vitro* anticancer activity and SAR studies of arylated imidazo[1,2-*a*]pyrazine-coumarin hybrids. RSC Adv. 2015;5:37887-95.

Gomha SM, Salaheldin TA, Hassaneen HME, Abdel-Aziz HM, Khedr MA. Synthesis, characterization and molecular docking of novel bioactive thiazolyl-thiazole derivatives as promising cytotoxic antitumor drug. Molecules. 2015;21(1):E3, doi: 10.3390/molecules21010003.

Gregoretti IV, Lee YM, Goodson HV. Molecular evolution of the histone deacetylase family: functional implications of phylogenetic analysis. J Mol Biol. 2004;338:17-31.

Hao YM. 2-Chloro-5-nitrobenzaldehyde thiosemicarbazone. Acta Cryst. 2010;66:o2528.

Hernandez W, Paz J, Carrasco F, Vaisberg A, Spodine E, Richter R, et al. Synthesis, characterization, and *in vitro* cytotoxic activities of benzaldehyde thiosemicarbazone derivatives and their palladium(II) and platinum(II) complexes against various human tumor cell lines. Bioinorg Chem Appl. 2008;2008: Article ID 690952.

Hernandez W, Paz J, Carrasco F, Vaisberg A, Manzur J, Spodine E, et al. Synthesis and characterization of new palladium(II) complexes with ligands derived from furan-2-carbaldehyde and benzaldehyde thiosemicarbazone and their *in vitro* cytotoxic activities against various human tumor cell lines. Z Naturforsch B Chem Sci. 2010;65:1271-8.

Holiyachi M, Shastri SL, Chougala BM, Shastri LA, Joshi SD, Dixit SR, et al. Design, synthesis and structure-activity relationship study of coumarin benzimidazole hybrid as potent antibacterial and anticancer agent. Chemistry Select. 2016;1:4638-44.

Hubschwerlen C, Specklin JL, Sigwalt C, Schroeder S, Locher HH. Design, synthesis and biological evaluation of oxazolidinone-quinoline hybrids. Bioorg Med Chem. 2003;11:2313-9.

Ilies M, Dowling DP, Lombardi PM, Christianson DW. Synthesis of a new trifluoromethylketone analogue of l-arginine and contrasting inhibitory activity against human arginase I and histone deacetylase 8. Bioorg Med Chem Lett. 2011;21:5854-8.

Jarrahpour A, Fathi J, Mimouni M, Ben Hadda T, Sheikh J, Chohan ZH, et al. Petra, Osiris and molinspiration (POM) together as a successful support in drug design: antibacterial activity and biopharmaceutical characterization of some azo Schiff bases. Med Chem Res. 2011;19:1-7.

Kaishi NK. Synthetic retarders for photographic emulsions. IV. Photographic properties of thiosemicarbazone derivatives. Ind Chem Sect. 1953;56:373-5.

Kamal A, Adil SF, Tamboli JR, Siddardha B, Murthy USN. Synthesis of coumarin linked naphthalimide conjugates as potential anticancer and antimicrobial agents. Lett Drug Des Discov. 2009;6:201-9.

Kawai K, Nagata N. Metal-ligand interactions: An analysis of zinc binding groups using the Protein Data Bank. Eur J Med Chem. 2012;51:271-6.

Klenkar J, Molnar M. Natural and synthetic coumarins as potential anticancer agents. J Chem Pharm Res. 2015;7:1223-38.

Kouzarides T. Chromatin modifications and their functions. Cell. 2007;128:693-705.

Li H, Wang X, Xu G, Zeng L, Cheng K, Gao P, et al. Synthesis and biological evaluation of a novel class of coumarin derivatives. Bioorg Med Chem Lett. 2014; 24:5274-8.

Lipinski CA, Lombardo F, Dominy BW, Feeney PJ. Experimental and computational approaches to estimate solubility and permeability in drug discovery and development settings. Adv Drug Deliv Rev. 2001; 46:3-26.

Liu MM, Chen XY, Huang YQ, Feng P, Guo YL, Yang G, et al. Hybrids of phenylsulfonylfuroxan and coumarin as potent antitumor agents. J Med Chem. 2014;57: 9343-56.

Luo G, Chen M, Lyu W, Zhao R, Xu Q, You Q, et al. Design, synthesis, biological evaluation and molecular docking studies of novel 3-aryl-4-anilino-2*H*-chromen-2-one derivatives targeting ERα as anti-breast cancer agents. Bioorg Med Chem Lett. 2017;27: 2668-73.

Lv PC, Zhou CF, Chen J, Liu PG, Wang KR, Mao WJ, et al. Design, synthesis and biological evaluation of thiazolidinone derivatives as potential EGFR and HER-2 kinase inhibitors. Bioorg Med Chem. 2010;18:314-9.

Madsen AS, Kristensen HM, Lanz G, Olsen CA. The effects of various zinc binding groups on inhibition of histone deacetylases 1-11. Chem Med Chem. 2014;9:614-26.

Mendoza-Merono R, Menedez-Taboada L, Fernandez-Zapico E, Garcia-Granda S. 1-(Biphenyl-4-ylmethylidene)thiosemicarbazide monohydrate. Acta Cryst. 2010;66:o1029.

Methot JL, Chakravarty PK, Chenard M, Close J, Cruz JC, Dahlberg WK, et al. Exploration of the internal cavity of histone deacetylase (HDAC) with selective HDAC1/HDAC2 inhibitors (SHI-1:2). Bioorg Med Chem Lett. 2008;18:973-8.

Morsy SA, Farahat AA, Nasr MNA, Tantawy AS. Synthesis, molecular modeling and anticancer activity of new coumarin containing compounds. Saudi Pharm J. 2017, http://dx.doi.org/10.1016/j.jsps.2017.02.003.

Mosmann T. Rapid colorimetric assay for cellular growth and survival: Application to proliferation and cytotoxicity assays. J Immunol Methods. 1983;65:55-63.

Nofal ZM, Soliman EA, Abd El-Karim S, El-Zahar M I, Srour AM, Sethumadhavan S, et al. Synthesis of some new benzimidazole-thiazole derivatives as anti-cancer agents. J Heterocycl Chem. 2014;51:1797-806.

Oberling C, Guerin M. The role of viruses in the production of cancer. Adv Cancer Res. 1954;2:353-423.

Pahontu E, Fala V, Gulea A, Poirier D, Tapcov V, Rosu T. Synthesis and characterization of some new Cu(II), Ni(II) and Zn(II) complexes with salicylidene thiosemicarbazones: Antibacterial, antifungal and in vitro antileukemia activity. Molecules. 2013;18:8812-36.

Pangal AA, Shaikh JA, Khan EM. Current developments of C3-substituted coumarin hybrids as anti-cancer agents. Int J Pharm Sci Rev Res. 2017;42:161-8.

Pasha FA, Muddassar M, Beg Y, Cho SJ. DFT-based de novo QSAR of phenoloxidase inhibitors. Chem Biol Drug Des. 2008;71:483-93.

Piens N, De Vreese R, De Neve N, Hecke KV, Balzarini J, De Kimpe N, et al. Synthesis of novel thymine-β-lactam hybrids and evaluation of their antitumor activity. Synthesis. 2014;46:2436-44.

Pingaew R, Prachayasittikul S, Ruchirawat S, Prachayasittikul V. Synthesis and cytotoxicity of novel 4-(4-(substituted)-1*H*-1,2,3-triazol-1-yl-*N*-phenethylbenzenesulfonamides. Med Chem Res. 2014a;23:1768-80.

Pingaew R, Saekee A, Mandi P, Nantasenamat C, Prachayasittikul S, Ruchirawat S, et al. Synthesis, biological evaluation and molecular docking of novel chalcone-coumarin hybrids as anticancer and antimalarial agents. Eur J Med Chem. 2014b;85:65-76.

Prashanth T, Thirusangu P, Avin BRV, Ranganatha VL, Prabhakar BT, Khanum SA. Synthesis and evaluation of novel benzophenone-thiazole derivatives as potent VEGF-A inhibitors. Eur J Med Chem. 2014; 87:274-83.

Riveiro ME, De Kimpe N, Moglioni A, Vazquez R, Monzor F, Shayo C, et al. Coumarins: Old compounds with novel promising therapeutic perspectives. Curr Med Chem. 2010;17:1325-38.

Rodolpho CD, Andrade CH. Assessing the performance of 3D pharmacophore models in virtual screening: How good are they?. Curr Top Med Chem. 2013;13: 1127-38.

Romagnoli R, Baraldi PG, Salvador MK, Camacho ME, Balzarini J, Bermejo J, et al. Anticancer activity of novel hybrid molecules containing 5-benzylidene thiazolidine-2,4-dione. Eur J Med Chem. 2013;63: 544-57.

Rouf A, Tanyeli C. Bioactive thiazole and benzothiazole derivatives. Eur J Med Chem. 2015;97:911-27.

Salisbury CM, Cravatt BF. Activity-based probes for proteomic profiling of histone deacetylase complexes. Proc Natl Acad Sci USA. 2007;104:1171-6.

Sandhu S, Bansal Y, Silakari O, Bansal G. Coumarin hybrids as novel therapeutic agents. Bioorg Med Chem. 2014;22:3806-14.

Sashidhara KV, Kumar A, Kumar M, Sarkar J, Sinha S. Synthesis and in vitro evaluation of novel coumarin-chalcone hybrids as potential anticancer agents. Bioorg Med Chem Lett. 2010;20:7205-11.

Seidel C, Schnekenburger M, Zwergel C, Gaascht F, Mai A, Dicato M, et al. Novel inhibitors of human histone deacetylases: Design, synthesis and bioactivity of 3-alkenoylcoumarines. Bioorg Med Chem Lett. 2014; 24:3797-801.

Sheeja KR, Kuttan G, Kuttan R. Cytotoxic and antitumour activity of Berberin. Amala Res Bull. 1997; 17:73-6.

Shitre GV, Bhosale RS, Karhale DS, Sujitha P, Kumar CG, Krishna KV, et al. Synthesis and biological evaluation of novel α-aminophosphonate derivatives possessing thiazole-piperidine skeleton as cytotoxic agents. Chem Biol Interface. 2014;4:48-57.

Siddiqui N, Arshad M, Khan S. Synthesis of some new coumarin incorporated thiazolyl semicarbazones as anticonvulsants. Acta Pol Pharm Drug Res. 2009;66:161-7.

Sreekanth T, Kavitha N, Shyamsunder A, Rajeshwar Y, Sabhassomalingappa K. Synthesis, characterization, in vitro cytotoxic and antioxidant activities of novel coumarin thiazolyl derivatives. Int J Pharm Educ Res. 2014;1:29-35.

Srimanth K, Rao VR, Krishna DR. Synthesis and evaluation of anticancer activity of some imidazothiazolyl, imidazobenzothiazolyl and dihydroimidazothiazolyl coumarins. Arzneimittelforschung. 2002;52: 88-92.

Stahl M, Rarey M. Detailed analysis of scoring functions for virtual screening. J Med Chem. 2001;44: 1035-42.

Sumangala V, Poojary B, Chidananda N, Arulmoli T, Shenoy S. Synthesis and biological evaluation of 2,4-disubstituted-[1,3]-thiazoles. Chem Pharm Res. 2012; 4:4979-87.

Tay F, Erkan C, Sariozlu N Y, Ergene E, Demirayak S. Synthesis, antimicrobial and anticancer activities of some naphthylthiazolylamine derivatives. Biomed Res. 2017;28:2696-703.

Tsurkan AA, Gromova ZF, Rudzit EA, Neshchadim GN, Kulikova DA. Synthesis of biologically active cyclopenteno[d]selenazole derivatives and their thio analogs. Khim-Farm Zh. 1982;16:692-5.

Tung TT, Oanh DT, Dung PT, Hue VT, Park SH, Han BW, et al. New benzothiazole/thiazole-containing hydroxamic acids as potent histone deacetylase inhibitors and antitumor agents. Med Chem. 2013;9:1051-7.

Ursu O, Rayan A, Goldblum A, Oprea T. Understanding drug-likeness. WIREs Comput Mol Sci. 2011;1: 760-81.

Vaarla K, Kesharwani RK, Santosh K, Vedula RR, Kotamraju S, Toopurani MK. Synthesis, biological activity evaluation and molecular docking studies of novel coumarin substituted thiazolyl-3-aryl-pyrazole-4-carbaldehydes. Bioorg Med Chem Lett. 2015;25:5797-803.

Valizadeh H, Gholipur H, Shockravi A. Microwave assisted synthesis of coumarins via potassium carbonate catalyzed Knoevenagel condensation in 1-n-butyl-3-methylimidazolium bromide ionic liquid. J Heterocycl Chem. 2007;44:867-70.

Veber DF, Johnson SR, Cheng HY, Smith BR, Ward KW, Kopple KD. Molecular properties that influence the oral bioavailability of drug candidates. J Med Chem. 2002;45:2615-23.

Weerasinghe SV, Estiu G, Wiest O, Pflum MK. Residues in the 11 Å channel of histone deacetylase 1 promote catalytic activity: Implications for designing isoform-selective histone deacetylase inhibitor. J Med Chem. 2008;51:5542-51.

Wolber G, Langer T. LigandScout: 3D pharmacophores derived protein-bound ligands and their use as virtual screening filters. J Chem Inf Comp Sci. 2005; 45:160-9.

Yi W, Dubois C, Yahiaoui S, Haudecoeur R, Belle C, Song H, et al. Refinement of arylthiosemicarbazone pharmacophore in inhibition of mushroom tyrosinase. Eur J Med Chem. 2011;46:4330-5.

Yuan JW, Wang SF, Luo ZL, Qiu HY, Wang PF, Zhang X, et al. Synthesis and biological evaluation of compounds which contain pyrazole, thiazole and naphthalene ring as antitumor agents. Bioorg Med Chem Lett. 2014;24:2324-8.

Zain J, Kaminetzky D, O'Connor OA. Emerging role of epigenetic therapies in cutaneous T-cell lymphomas. Expert Rev Hematol. 2010;3:187-203.

Zhang L, Yao YC, Gao MY, Rong RX, Wang KR, Li XL, et al. Anticancer activity and DNA binding property of the trimers of triphenylethylene-coumarin hybrids. Chin Chem Lett. 2017;27:1708-16.

Zhang W, Li Z, Zhou M, Wu F, Hou X, Luo H, et al. Synthesis and biological evaluation of 4-(1,2,3-triazol-1-yl)coumarin derivatives as potential antitumor agents. Bioorg Med Chem Lett. 2014;24:799-807.